NORDIC STEEL 2024
The 15th Nordic Steel Construction Conference,
June 26–28, 2024, Luleå, Sweden

Steel-timber composite structures with semi-rigid beam-to-column joints: Overview and perspectives towards a design for disassembly & reusability

Alper Turgut*,[a], Hervé Degée[a], José Henriques[a]

[a]Construction Engineering Research Group, University Hasselt, Belgium
alper.turgut@uhasselt.be, herve.degee@uhasselt.be, jose.gouveiahenriques@uhasslet.be

ABSTRACT

Composite structures, which combine two or more complementary materials, have long been utilized in the construction sector for their structural efficiency and economic benefits. Due to the latest advancements in timber manufacturing technology, use of timber in structural composite applications has gained popularity, given its environmental advantages in reducing the carbon footprint of the buildings. Particularly, Timber-Concrete Composite (TCC) structures have gained significant popularity over the past two decades. However, the use of steel in a composite framework with timber is a relatively new concept. Especially considering steel's greater ductility compared to the concrete, suitability for reuse, and its superior mechanical properties, steel-timber composite (STC) structures hold significant potential. While there are some studies on steel-timber flooring solutions, the majority focuses on the connections between steel beams and timber panels. Few works explore the advantages of moment beam-to-column joints in enhancing bending moment distribution and reducing deflections in STC beams. However, none of the configurations proposed in these studies fully integrate the disassembly and reusability concept. This study aims to provide an overview of existing configurations in the literature and evaluate their adaptability for the disassembly and reusability concept by offering a mechanical assessment of various solutions available in the literature. Initial assessments involved a comparative analysis of existing configurations. A collection of investigated STC beam-to-columns joints are evaluated for their mechanical behavior such as: rotational stiffness, rotation capacity, bending moment capacity, ductility and associated failure modes. Subsequently, an evaluation of existing solutions in terms of disassembly and reusability is conducted, leading to the identification of a future design need in this regard. Finally, a Finite Element Analysis (FEA) is conducted to further complement the analysis.

Keywords: steel-timber composite, semi rigid, demountable, cross-laminated timber (CLT)

1 INTRODUCTION

Buildings are responsible for 40% of global greenhouse gas emissions (1) and 50% of raw material consumption (2). Consequently, there has been a growing demand for urgent environmental change in the construction sector. The industry is looking for innovative strategies to integrate sustainable solutions into structural design. To meet this demand, in recent years, timber has gained popularity as an eco-friendly alternative to traditional construction materials.

Recent advancements in timber manufacturing technology have significantly improved the mechanical properties of timber. The development of engineered wood products (EWP) has particularly positioned timber as one of the most promising alternative materials for replacing traditional materials in the construction sector. Therefore, the use of timber in a composite form with other construction materials has emerged as one of the innovative construction techniques over the last two decades. Timber-concrete composite (TCC) structures are a leading example of timber's application in such systems. However, the concept of steel-timber composites (STC) is a relatively new idea. Given steel's superior ductility compared to concrete, its suitability for reuse, and superior

mechanical properties make these composite structures highly promising. Especially, the integration of timber's environmentally friendly character with the strong and ductile mechanical properties of steel shows the potential for such composites to enable the construction of multi-story buildings that can reduce carbon footprint of the building while providing sufficient mechanical performance.
In STC structures, one of the most common use is combining steel beams and columns with timber flooring panels. In such applications, the critical design principle lies in the connections. The connections of such systems are studied by various researchers (3,4). However, studies investigating STC beam-to-column joints in the semi-rigid cruciform are relatively limited. There are three fundamental connections in a STC beam-to-column joint (*Fig. 1*). The first is the connection between the steel beam and the steel column, which has been extensively studied in numerous works from the past to the present. The second connection is between the steel beam and the timber panel, activating the composite action through shear connections. This connection has become a trend research topic in recent years, evolving through design concepts proposed by various researchers (5,6). The third connection is the connection between timber panels. In previous studies, the significant impact of slab-to-slab connections on moment and rotation capacities is demonstrated for different type of composite joints (7,8). However, a comprehensive study that examines these connections in detail within the STC context and evaluates them from the perspective of disassembly and reusability concepts is yet to be conducted. In this study, the existing STC beam-to-column slab-to-slab connections are mechanically evaluated in terms of their potential, and a future perspective is presented. Afterwards, a selected joint design was numerically modeled, and the behavior of the joint is examined in detail.

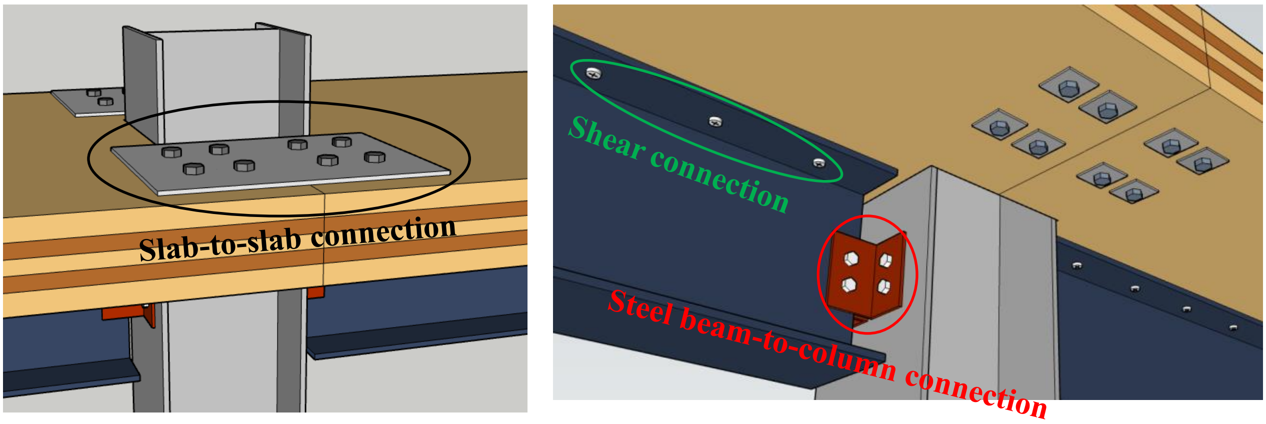

Fig. 1. Steel-timber composite beam-to-column joint

2 EXISTING BEAM-TO-COLUMN JOINT CONFIGURATIONS

STC joint configurations in the literature are categorized into 5 groups based on the type of slab-to-slab connection (*Fig. 2*). These vary in terms of shape and size. In the experimental studies, cross-laminated timber (CLT) is used as the timber slab, and S16x100 mm coach screws are used as the shear connector in almost all specimens. However, as steel beam-to-column connection, four different connections are used which are extended end plate, flush end plate, fin plates and angle web cleats.

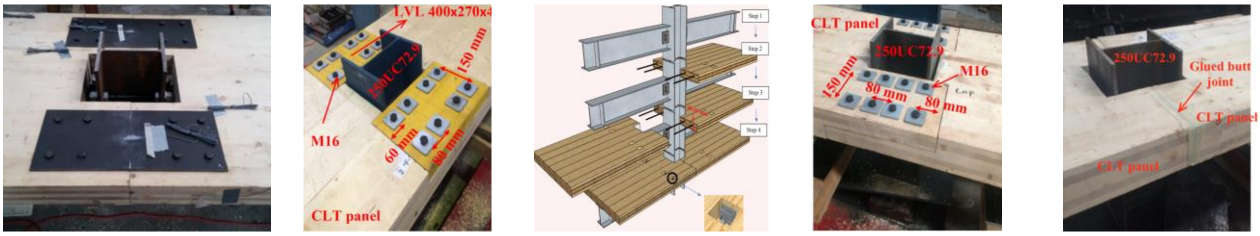

a) b) c) d) e)

Fig. 2. Existing STC beam-to-column slab-to-slab connections; a) steel cover plates (9), b) LVL (laminated veneer lumber) cover panels (10), c) anchored steel rods (11), d) half-lap connection (12), e) glued butt connection (13).

The steel cover plates (*Fig. 2a)* are the most commonly used connection type as slab-to-slab connection across the column. In this type of connection, the load is transferred by connected steel cover plates and bolts across the CLT panels. The steel cover plates are used in three ways; rectangular plates on the top of CLT panels, additional plates on the bottom, and dog-bone shaped plates as an alternative.

The second configuration shares a similar working principle with the steel cover plate, but LVL panels are used instead of steel plates. The top parts of both CLT panels are cut to the depth of the LVL cover panels to be placed, and the inserted LVL panels is connected to the CLT panels by bolts and washers (*Fig. 2b)*. The load transfer between CLT panels is achieved through LVL panels and bolts.

Another connection method is inserting steel rods into the CLT panels. In this method, CLT panels are connected through steel rods inserted within them. The steel rods are anchored into a pocket cut from the surface of the CLT with the aid of grout (*Fig. 2c)*. In this type of connection, the main load transfer between CLT panels is facilitated by steel rods.

Half-lap connection is another method used as slab-to-slab connection. Two CLT panels are cut to overlap each other. Then, the panels are overlaid on top of each other and connected with bolts and washers that pass through both panels (*Fig. 2d)*. In this method, the primary load-transfer mechanism is provided by the bolts.

Compared to the other four connection configurations, the most basic form is gluing the CLT panels to each other. In this configuration, without using any additional connection elements, the panels are glued together (*Fig. 2e)*.

3 MECHANICAL ASSESMENT OF EXISTING CONFIGURATIONS

In this section, based on experimental results in the literature, the configurations are examined in terms of moment capacity, rotation at peak moment, rotational stiffness, ductility, and failure modes, and the mechanical performance of the configurations is compared. An example of the test setup used in all joint tests under negative bending moment is illustrated in *Fig. 3*.

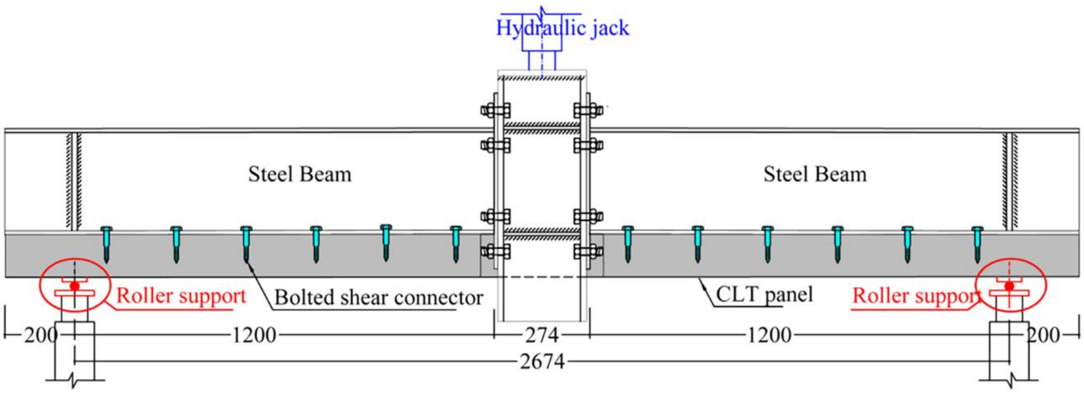

Fig. 3. Test setup (9)

From the experimental studies, a set of specimens are chosen to enable a comparative analysis of various slab-to-slab connections and they are listed in *Table 1*. The specimen names are formatted as X-Y, where 'X' represents the slab-to-slab connection, and 'Y' for the steel beam-to-column connection. For instance, in the 'LVL-F1' specimen, an LVL cover panels are used as the slab-to-slab connection, while a flush end plate is used as steel beam-to-column connection. As an exception, in the 'ST-F1-C800' and 'GL-F1-C800' specimens, 'C800' represents a CLT slab width of 800 mm, in contrast to the 1000 mm width used in the other specimens.

Table 1. Experimental results of the specimens

Reference	Specimen	Slab-to-slab connection	Steel beam-to-column connection	Slab-to-slab connector dimensions (mm)	M_{peak} (kNm)	θ_{peak} (mRad)	Rotational Stiffness (kNm/mRad)	Ductility index (Δ_u/Δ_y)
(13)	B-F	-	Flush End Plate	-	120	39.5	12.8	8.1
(13)	ST-F1	Steel cover plates	Flush End Plate	400x300x6	244	72.2	16.2	6.36
(13)	ST-F2	Double steel cover plates	Flush End Plate	300x250x6	255	86.4	26.7	8.75
(10)	HL-F1	Half-lap	Flush End Plate	-	209	41.2	14.9	4.49
(10)	LVL-F1	LVL panels	Flush End Plate	400x270x45	173	39.7	15.7	4.72
(10)	LVL-F2	LVL panels	Flush End Plate	600x270x45	188	49.8	16	5.58
(12)	ROD-F1	Steel rods	Flush end plate	D16, 4 rods	208	28.9	17.6	4.17
(13)	ST-F1-C800	Steel cover plates	Flush End Plate	400x270x6	217	45.9	14.7	4.78
(13)	GL-F1-C800	Glued butt	Flush End Plate	-	135	64.5	38.7	
(9)	B-E	-	Extended End Plate	-	210.8	44.9	55	
(9)	ST-E1	Steel cover plates	Extended End Plate	600x250x6	305.4	48.2	121	
(9)	ST-E2	Dog bone steel cover plates	Extended End Plate	600x250x6	297.8	47.2	115	
(9)	ROD-E1	Steel rods	Extended End Plate	D16, 4 rods	250.3	22.2	125	
(9)	ROD-E2	Steel rods	Extended End Plate	D12, 4 rods	276	41.5	85	
(14)	B-W	-	Web angles (250 mm)	-	28.8	104.2	0.6	3.44
(14)	ST-W1	Steel cover plates	Web angles (150 mm)	400x300x6	85.5	98.6	3.15	8.85
(14)	ST-W2	Steel cover plates	Web angles (250 mm)	400x300x6	118.3	83.1	4	11
(14)	LVL-W1	LVL panels	Web angles (150 mm)	600x300x45	48.5	71.6	2.2	8.5
(11)	ROD-W1	Steel rods	Web angles (150 mm)	D16, 4 rods	76.72	71.6	3.3	3.11
(11)	ROD-W2	Steel rods	Web angles (150 mm)	D16, 6 rods	96.45	43.1	2.9	2.4
(15)	ST-F1	Steel cover plates	Fin plates (150 mm)	400x300x6	67.5	70	2.34	3.78
(15)	LVL-F1	LVL panels	Fin plates (150 mm)	600x300x45	52	81	2	4.76
(11)	ROD-F1	Steel rods	Fin plates (150 mm)	D16, 4 rods	55.7	83.1	2.49	2.82

3.1 Moment Capacity

The moment capacity represents the peak moment value at the face of the columns. To calculate this moment, the reaction force from the roller support is multiplied by the distance between the roller support and the face of the column. A significant increase in moment capacity observed in all specimens compared to their bare steel counterparts, except for joints with glued butt connection.

From *Table 1*, it is observed that in all cases, specimens with steel cover plates achieved the highest moment capacity. The sole exception to this observed in a steel rod configuration where two additional rods are directly connected from the CLT to the steel column (ROD-W2), resulting in 12% higher moment value compared to the equivalent specimen with steel cover plates. Additionally, using double or dog-bone shaped steel cover plates have neglectable effect on the peak moment value. Joints with steel rods and half-lap connections share the second rank in the moment capacity. The half-lap connection is used in only one specimen (HL-F1), and it achieved the same peak moment value as the identical specimen with steel rods (ROD-F1). Directly connecting two additional rods to the column significantly increases the peak moment capacity in the specimens with steel rods, whereas increasing the diameter of the rods resulted in a decrease in peak moment.
In specimens with LVL cover panels, a significant increase in moment capacity is observed compared to their bare steel counterparts, yet the moment capacity contribution remains substantially below that of the first three types of connections. It is observed that increasing the length of the LVL cover panels results in a slight increase in the peak moment value.
Finally, the moment capacity of the joints with glued butt connections remained the same as the bare steel joints.

3.2 Rotation at Peak Moment

The rotation values in all specimens is measured at the same location as the moment, the face of the column. The joint's rotation is calculated by dividing the column's vertical displacement by the beam's length (Δ/l_b). In almost all specimens, composite joints demonstrated a significant increase in rotation at peak moment values compared to bare steel joints.
The joint with glued butt connection using 800 mm CLT (GL-F1-C800) achieved a 40% higher rotation value than its equivalent specimen with steel cover plates (ST-F1-C800). In specimens with flush and extended end plate, or angle web cleats, joints with the steel cover plates reached a higher rotation at peak moment compared to the other specimens. In specimens with fin plates, configurations using LVL cover panels and steel rods achieved a higher rotation value than those with steel cover plates. However, in a general assessment of the rotation performance among slab-to-slab connections, steel cover plates and glued butt connections showed the best performance, while specimens with LVL cover panels, steel rods, and half-lap connections showed relatively lower performance.
The use of double side steel cover plates instead of single results a 20% increase in rotation at peak moment, while using dog-bone shaped steel cover plates has a negligible impact. Increasing the length of the LVL cover panels significantly enhances the rotation capacity. Lastly, increasing the number or diameter of steel rods causes a dramatic decrease in the rotation at peak moment.

3.3 Rotational Stiffness

Initial rotational stiffness is calculated by determining the slope of the moment-rotation curve at the points where the specimen reaches 40% and 10% of its maximum load. In all composite joints, a significant increase in rotational stiffness is observed compared to bare steel joints.
The greatest increase in rotational stiffness observed in glued butt joints. It is followed by joints with steel rods, steel cover plates, LVL cover panels, and half-lap connections, respectively.

3.4 Ductility

The ductility index is defined as $u = \Delta_u/\Delta_y$, where Δ_u and Δ_y represent the column's vertical displacements corresponding to the peak and yield loads, respectively. In specimens with extended end plates, due to the lack of information regarding the ductility index or the load-displacement curve, the results are not included in the evaluation.
In almost all joints with flush end-plates, the ductility index of composite joints showed a lower ductility value than the identical bare steel joints. The only exception to this is the joint with double side steel cover plates (ST-F2), which showed only 8% increase in ductility. On the other hand, when comparing bare steel (B-W) and steel cover plates (ST-W2) joints with 250 mm angle web cleats as beam-to-column connector, it is observed that the composite joint with the steel cover plates achieved

a ductility index more than three times higher than that of the bare steel joint. This indicates that when less rigid steel beam-to-column connections are used, composite joints hold a potential for great increase in ductility.

In an analysis of the general trend, it is observed that steel cover plates achieve the highest ductility index values in comparison to the other configurations. This is followed in order by LVL cover panels, half-lap connections, and steel rods. In the specimens with glued butt connections, due to sudden load drops resulting from fractures in the glue between the two panels, it was not possible to determine a discernible yield point to measure the ductility index. Consequently, it is concluded that they have the lowest potential for ductility among the examined configurations.

Moreover, using double side steel cover plates significantly increases the ductility index. Increasing the length of the LVL cover panels contributes moderately to the ductility index. In specimens with steel rods, adding two extra steel rods results in a considerable decrease in the ductility index.

3.5 Failure Modes

In the experimental studies, mixed failure mechanisms were observed. The most prominent among these are shown in *Fig. 4*.

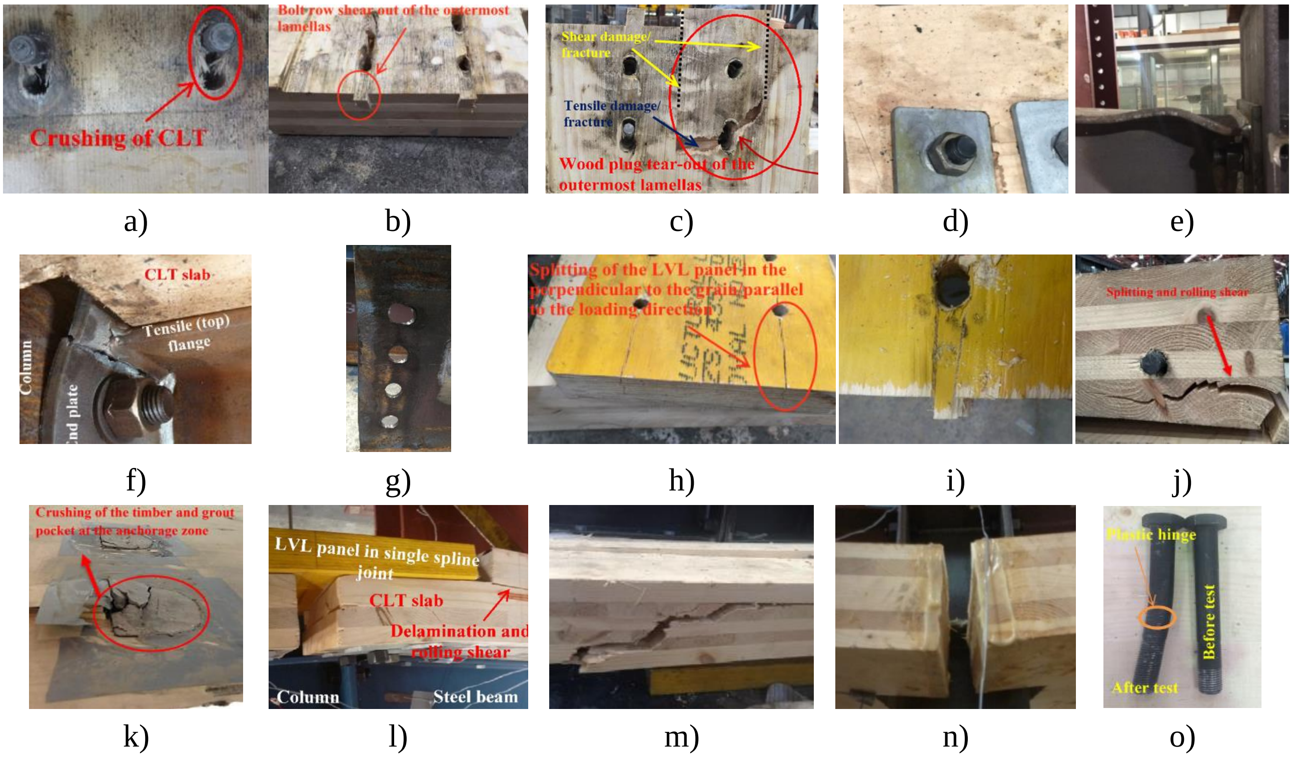

Fig. 4. Outstanding failure mechanisms; a) crushing of timber near the bolts, b) row shear of the timber, c) plug shear of the timber, d) crushing of the timber beneath the washers, e) buckling of the steel flange, f) end plate fracture, g) bearing of the beam web, h) splitting of the LVL cover panel, i) row shear of the LVL cover panel, j) splitting and rolling shear of the CLT, k) crushing of the timber and grout at the pocket, l) delamination and rolling shear of the CLT, m) rolling shear of the CLT, n) fracture of the glue, o) plastic hinge on the bolts (10-14).

In joints with steel cover plates, except those with extended end-plates, as beam-to-column connectors, CLT panel damage is observed in all specimens. This damage appears as crushing around the bolts connecting the steel cover plate to the CLT panel (*Fig. 4a*), row shear (*Fig. 4b*), plug shear (*Fig. 4c*), and crushing beneath the washer (*Fig. 4d*). Apart from timber damage, excessive rotation of the beam and compressive buckling of the steel beam flange (*Fig. 4e)* is observed in all specimens. End plate fracture (*Fig. 4f)* is also observed in some specimens. Besides buckling of the steel flange and end plate fracture, bearing of the steel beam (*Fig. 4f)* is also noted in some tests including joints with steel cover plates and steel rods.

In specimens where slab continuity is achieved with LVL cover panels, crushing of the CLT and LVL panels around the bolts connecting the LVL panel to the CLT is observed after all experiments. Additionally, crushing of the CLT panel beneath the washer is noted. In specimens with relatively shorter LVL panels, row shear (*Fig. 4i*), and splitting (*Fig. 4h)* in the LVL panel and plug shear, delamination (*Fig. 4l)* of the CLT panel is also observed. Increasing the length of the LVL overcomes these failure modes, but crushing of the CLT around the bolts remains the primary failure mode. Furthermore, in specimens using web angles and fin plates, rolling shear failures (*Fig. 4m)* in the CLT is also observed.

In specimens with steel rods, the most commonly observed failure mode is the crushing of the grout concrete in the rod anchorage pockets and the surrounding CLT panel (*Fig. 4k)*. Additionally, plug shear, splitting and rolling shear (*Fig. 4j)* of the CLT is observed. Furthermore, in some specimens with end plates, end plate fracture and compressive buckling of the steel beam flange is noted.

In joints with half-lap connection, plug shear and row shear of the CLT, crushing of the CLT near the bolts, and crushing of the CLT beneath the washers are observed.

In joints where CLT slabs are glued, a glue fracture occurred first (*Fig. 4n)*, followed by an end plate fracture.

Apart from these, some studies have discussed disassembly (9-11), leading to mentions of plastic deformation in the bolts of slab-to-slab connections (*Fig. 4n)*. While significant plastic deformation in these bolts is noted, it is stated that this does not hinder disassembly. However, there is no clear information provided on the disassembly method (destructive or non-destructive) and on which specimens exhibited plastic deformation in the bolts.

3.6 Comparison of Existing Configurations

Based on the results of the experimental studies, the mechanical performances of slab-to-slab connections in terms of peak moment, corresponding rotation, rotational stiffness, and ductility are ranked in Table 2. Even though there are some exceptions that disrupt this order, the ranking is made according to the general trend.

Table 2. Comparison of the configurations

Rank	Moment capacity	Corresponding rotation	Rotational stiffness	Ductility
1	Steel cover plates	Glued butt connection	Glued butt connection	Steel cover plate
2	Steel rods ≈ Half-lap connection	Steel cover plates	Steel rods	LVL panels
3	LVL panels	LVL panels ≈ Steel rods ≈ Half-lap connection	Steel cover plates	Half-lap connection
4	Glued butt connection		LVL panels	Steel rods
5			Half-lap connection	Glued butt connection

The compared STC beam-to-column joint configurations are examined from the perspective of demountability and reusability. It appears that joints with glued butt and anchored steel rod connections cannot be demountable with non-destructive methods. While disassembly and reusability of joints with steel cover plates, LVL cover panels, and half-lap connections seem feasible, the significant damage induced in the CLT panel in failure modes presents a major obstacle to reusability. Also, the demountability of these connections can vary depending on the level of plastic deformation in the bolts. A shift of the failure mechanisms from timber and steel parts to the replaceable steel cover plates or LVL cover panels, holds significant potential for disassembly and reusability. However, this scenario is not observed in any tested specimen. Given the superior mechanical properties of connections with steel cover plates compared to those with LVL cover panels, and considering steel's ductile behaviour, designing a joint configuration that shifts the failure mode from the timber panel to the steel cover plates has yet to be developed.

4 FINITE ELEMENT ANALYSIS

In this section, a 3D non-linear finite element analysis (FEA) of a STC beam-to-column joint is presented for a more detailed examination and to validate the experimental results. The specimen chosen for the analysis involves steel cover plates as the slab-to-slab connection, selected for its superior mechanical performance and disassembly, reusability potential as mentioned in *Section 3*, and angle web cleats as steel beam-to-column connection, chosen for their common use in the market and ease of production. Therefore, ST-W1 specimen seen in *Table 1* is numerically modelled. A modelling approach similar to the previous studies is employed (16, 17). The material properties of the model are shown in *Table 3* and *Table 4.*

Table 3. Mechanical properties of CLT

	Parallel to the grain	Perpendicular to the grain	Longitudinal Shear	Rolling shear
Elastic Moduli (GPa)	11000	370	690	50
Strength (MPa)	36	4.6	6.9	0.5

Table 4. Mechanical properties of steel parts

Member	Yield stress (MPa)	Ultimate Stress (MPa)	Elastic moduli (GPa)
Bolts	640	800	200000
Screws	240	400	200000
Other steel parts	320	400	200000

For the material model of timber, Hill48 yield model (18) is used in *Abaqus* software. This model is not effective in capturing the tensile properties of timber, making it less optimal for capturing failure modes dependent on tension of the material, such as plug shear. On the other hand, as other observed failure modes related to timber are based on its compressive properties, it is anticipated that the joint model will yield good results in capturing these failure modes. To model the interaction between different components, the surface-to-surface contact option in *Abaqus* software is implemented. In the normal direction, hard contact option is used, while in the tangential direction, a penalty friction coefficient of 0.4 and 0.3 is used for steel-to-steel and steel-to-timber interactions, respectively. Considering computation speed, only a quarter of the joint is modelled benefiting from the symmetry of the problem. Similar to the experimental studies, displacement is measured at the column, and load is taken from roller supports. These values are converted into moment-rotation values using the distance between the roller support and the column face. *Fig. 5* shows the numerical model and the moment-rotation curve.

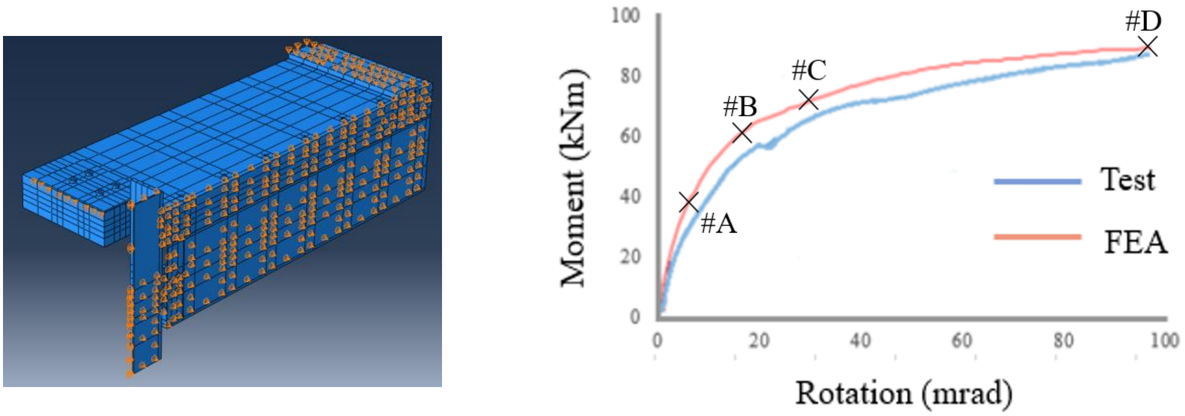

a) b)

Fig. 5. Finite element model (a) and the moment-rotation curve (b)

The model showed good accuracy in capturing the peak moment and corresponding rotation of the joint. However, the rotational stiffness value of the tested specimen is lower than the numerical model. The most possible reason for this is the unreliability of basing conclusions on only one test specimen, especially with a material as unpredictable as timber. The development of plastic strains in critical components is presented in *Table 5*.

Table 5. Plastic strains at critical components

	CLT	Bolts at slab-to-slab connection	Screws	Steel web	Steel cover plate
Plastic strain at point #A	0.012	0	0	0.015	0
Plastic strain at point #B	0.08	0.0007	0.003	0.08	0.004
Plastic strain at point #C	0.15	0.003	0.007	0.2	0.012
Plastic strain at point #D	0.64	0.027	0.018	0.5	0.05
Ultimate plastic strain of the material	0.01	0.1	0.2	0.2	0.2

For material modeling, a tri-linear material model is employed, and no damage mechanism is defined. Consequently, the materials continue to displace beyond their ultimate strain values after reaching their strength. *Fig. 6* illustrates the distribution of plastic strains at critical points showed in *Fig. 5b*.

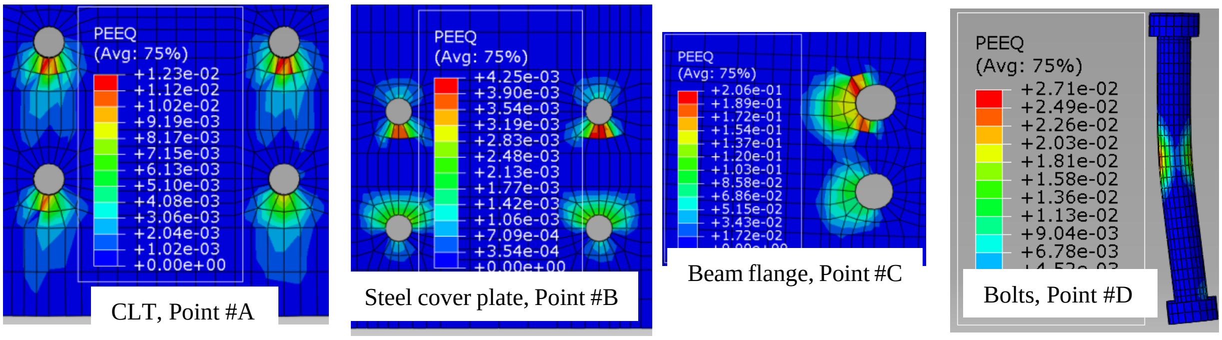

a) b) c) d)

Fig. 6. Distribution of plastic strains at the; (a) beginning of the local crushing of CLT, (b) beginning of the local plastic deformation in the steel cover plate, (c) beam flange capacity, (d) bolts at slab-to-slab connection after the test.

As a result of numerical analysis, in alignment with experimental findings, significant local crushing is observed in the CLT panel. The initial plastic strains throughout the joint were predominantly observed in the CLT panel. Furthermore, while screws, bolts and steel cover plate exhibited slight local plastic deformation, high levels of local plastic deformation were observed in the steel beam and the bolts within the beam.

5 CONCLUSIONS

In the framework of sustainable construction, innovative steel-timber composite (STC) flooring solutions hold numerous sustainability potentials, such as being lightweight, reducing the carbon footprint, and decreasing raw material usage. A comprehensive evaluation of the STC beam-to-column configurations is lacking in the literature. This study comparatively examined the mechanical properties of various slab-to-slab configurations and evaluated them in the context of deconstruction and reusability. Finally, a finite element analysis is conducted to provide a more in-depth examination of the joint behavior.

- STC beam-to-column joints exhibit a significant increase in moment capacity, corresponding rotation, and rotational stiffness compared to their bare steel counterparts. However, they can led to a reduction in ductility.
- Among the compared slab-to-slab connections, the steel cover plates provides the highest contribution to moment capacity and ductility, while the glued butt connection leads in the rotation at the peak moment and rotational stiffness.

– Using more rigid steel beam-to-column connections significantly enhance the joint's moment capacity and rotational stiffness values, but do not make a substantial contribution to the rotation at the peak moment and ductility.
– Configurations with steel rods and glued butt connections offer no potential for demountability with non-destructive methods while other configurations provide potential for dismantling and reuse. Demountability is dependent on the plastic deformation of the fasteners used in the connections. However, timber panel damage hinders reusability in all examined specimens.
– There is a need for a design that integrates disassembly and reusability by shifting the failure mechanism from steel beam and timber panels to the replaceable components, such as demountable connectors.

REFERANCES

1. UN Environment Program. Global Status Report, 2018.
2. DIRECTORATE-GENERAL Environment. Resource efficiency in the building sector – final report, 2014.
3. **Loss C., Davison B.** Innovative composite steel-timber floors with prefabricated modular components. *Eng. Struct. 132 (2017) pp. 695–713*
4. **Hassanieh A., Valipour H., Bradford M.** Experimental and numerical study of steel-timber composite (STC) beams. *J. Constr. Steel Res. 122 (2016), pp.* 367-378.
5. **Yang R. Y., Li H. T., Lorenzo R., Ashraf M., Sun Y. F., Yuan Q.** Mechanical behaviour of steel timber composite shear connections. *.Constr. Build. Mater. 258 (2020) 119605.*
6. **Ataei A., Chiniforush A. A., Bradford M., Valipour H.** Cyclic behaviour of bolt and screw shear connectors in steel-timber composite (STC) beams. *J. Constr. Steel Res. 161 (2019), pp.* 328-340.
7. **Ataei A., Bradford M., Valipour H., Liu X.** Experimental study of sustainable high strength steel flush end plate beam-to-column composite joints with deconstructable bolted shear connectors. *Eng. Struct. 123 (2016) pp. 124–140*
8. **Ataei A., Bradford M., Valipour H.** Experimental study of flush end plate beam-to-CFST column composite joints with deconstructable bolted shear connectors. *Eng. Struct. 99 (2015) pp. 616–630.*
9. **Ataei A., Valipour H., Bradford M., Chiniforush A. A.** Experimental study of steel-timber composite beam-to-column joints with extended end plates. *Constr. Build. Mater. 226 (2019) pp. 636-650.*
10. **Keipour N., Valipour H., Bradford M.** Steel-timber composite beam-to-column joints: Effect of connections between timber slabs. *J. Constr. Steel Res. 151 (2018), pp.* 132-145.
11. **Nouri F., Valipour H.** Semi-rigid partial-strength steel-timber composite (STC) connections with mechanically anchored steel rods. *J. Constr. Steel Res. 158 (2019), pp.* 560-575.
12. **Keipour N., Valipour H., Bradford M.** Structural behaviour of steel-timber versus steel-concrete composite joints with flush end plate. *Constr. Build. Mater. 262 (2020) 120885.*
13. **Keipour N., Valipour H., Bradford M.** Experimental study of steel-timber composite (STC) beam to steel column joints having a flush end-plate. *Engineering Structures 174 (2018), pp.* 906-918.
14. **Nouri F., Valipour H., Bradford M.** Structural behaviour of steel-timber composite (STC) beam-to-column connections with double angle web cleats subjected to hogging bending moment. *Engineering Structures 192 (2019), pp.* 1-17.
15. **Nouri F., Bradford M., Valipour H.** Steel–Timber Composite Beam-to-Column Connections with Shear Tab. *J. Struct. Eng. 145 (3) (2019), 04018268.*
16. **Nouri F., Valipour H., Bradford M.** Finite element modelling of steel-timber composite beam-to-column joints with nominally pinned connections. *Engineering Strucutres 201 (2019), 109864.*
17. **Nouri F., Valipour H.** Moment-rotation model for steel-timber composite connections with slab continuity steel rods. *J. Constr. Steel Res. 173 (2020), 106257.*
18. **Hill R.** A theory of the yielding and plastic flow of anisotropic metals. *Proc. R. Soc. A: Math. Phys. Eng. Sci. 193 (1948) pp. 281–297.*